Design Considerations for Magnetic Feedback Using Amplitude Modulation

Brian T. Irving and Milan M. Jovanović

Delta Products Corporation
Power Electronics Laboratory
P.O. Box 12173
5101 Davis Drive
Research Triangle Park, NC 27709 USA

***Abstract*- In off-line ac-dc and high-voltage dc-dc power supplies, galvanic isolation between the input and output is often implemented with optocoupler feedback. However, several disadvantages exist when implementing optocoupler feedback, such as a variable loop gain due to optocoupler tolerance and sensitivity to temperature, as well as a relatively high cost. An alternative to optocoupler feedback is to use magnetic feedback, which can be designed to have insensitivity to component tolerance, and good temperature stability. Although magnetic feedback has been in use for many years, a detailed analysis and clear design procedure has not been presented in the literature. This paper presents a thorough analysis of a magnetic feedback implementation, and provides a comprehensive design procedure which is verified on a 7-V/15-W experimental prototype.**

I. Introduction

Galvanic isolation between the input and output is a requirement of off-line ac-dc and high voltage dc-dc power supplies. In the power stage, galvanic isolation is typically achieved through use of a transformer. However, in order to provide regulation of the output, a galvanically isolated feedback loop is also required. Two commonly used isolation methods are primary-side control with optocoupler feedback [1]-[5] and secondary-side control, where the primary gate drive is provided through gate-drive transformers. The drawbacks of primary-side control with optocoupler feedback include variation of loop gain due to wide current transfer ratio *CTR*, sensitivity to both time and temperature, and a high cost. A drawback of secondary-side control is the need for an additional secondary-side supply voltage, often supplied by a separate "housekeeping" converter.

An alternative to primary-side control with optocoupler feedback and secondary-side control is to use magnetic feedback [1], [2], [6], [7]. Using a very small coupling transformer, a modulator, and a sample and hold circuit, a signal from the secondary side can be passed to the primary using either amplitude modulation (AM), or, frequency modulation (FM). A magnetic feedback circuit can be implemented either discretely, or, using an integrated IC [7].

Although it has been used in industry for many years, very few design details appear in the literature. The goal of this paper is to analyze an AM magnetic feedback implementation, and to provide a clear, step-by-step design procedure in order to optimize the circuit performance.

II. Principles of AM Magnetic Feedback

As shown in Fig. 1, magnetic feedback can be implemented using a small dc-dc transformer, which acts as both the modulator and demodulator, to pass error voltage V_{EA} from the secondary side to the primary side. The dc-dc transformer consists of a small coupling transformer and diode, which is excited by an external source to form the modulator, with its switching frequency equal to the modulator carrier frequency. The rectified output of the dc-dc transformer acts as a sample and hold circuit, or demodulator.

The coupling transformer (T_C) can be configured either as a forward-type or flyback-type converter, as shown in [6]. Both the carrier and sampling frequency, which are synchronized, can be equal to or higher than the power-stage switching frequency, depending on the desired volume of coupling transformer T_C and the desired loop performance. Generally, the loop gain of the converter is negatively impacted by the sampling delay of the demodulator.

A simplified block diagram of a general power stage with magnetic feedback implemented with a flyback-type dc-dc transformer is shown in Fig. 2. Error amplifier (EA) output V_{EA} represents the amplified difference between output voltage V_O and reference voltage V_{REF}. An isolated modulator is implemented by coupling transformer T_C, which is magnetized by current source i_C based on an external carrier signal. While current source i_C is on, diode D_{EA} is reversed biased, sampler switch S_H is off, and current i_C divides between magnetizing

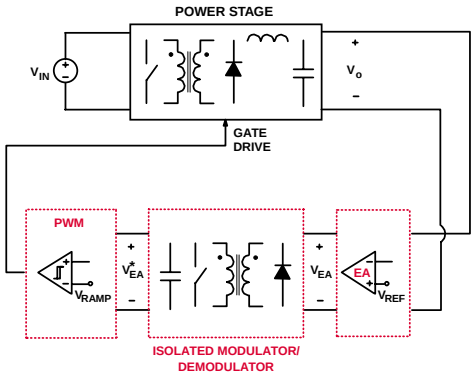

Fig. 1 A general power supply with isolated magnetic feedback.

978-1-4244-1874-9/08/$25.00 ©2008 IEEE

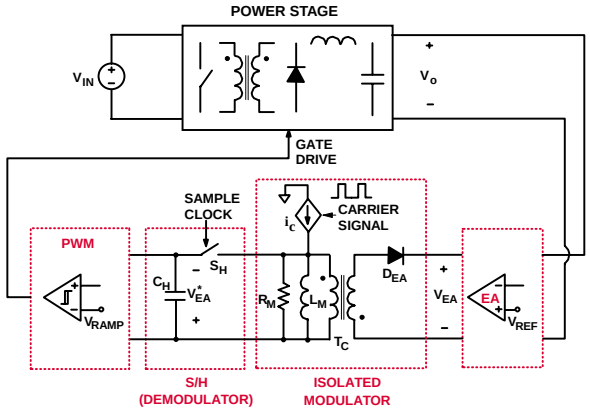

Fig. 2 A general power stage with amplitude modulated (AM) feedback and flyback dc-dc transformer.

inductance L_M and resistor R_M. Once current source i_C turns off, magnetizing current I_M forward biases diode D_{EA}, and error voltage V_{EA} is reflected to the primary side with a reverse polarity. Sampler switch S_H, which is synchronized to the modulator, turns on during the demagnetization period of coupling transformer T_C, and capacitor C_H holds the sampled error voltage V^*_{EA}, which is then compared at the pulse-width modulator (PWM) to periodic ramp voltage V_{RAMP} in order to generate the gate drive signal to the power stage.

Generally, coupling transformer T_C operates as a flyback converter because error voltage V_{EA} is sampled during the demagnetization period of coupling transformer T_C. As shown in [6], it is also possible to operate coupling transformer T_C as a forward converter, i.e., to sample error voltage V_{EA} during the magnetization period of coupling transformer T_C.

III. Analysis of AM Magnetic Feedback

An implementation of an AM magnetic feedback circuit applied to a forward converter with synchronous rectifiers and current mode control is shown in Fig. 3. Error amplifier EA is implemented with transconductance amplifier *TLV431* and with capacitor C_{KA} which allows *TLV431* to have a low output impedance at high frequencies. A dc-dc transformer is used as part of the modulator, and has both a flyback winding for sampling error voltage V_{EA}, and, a forward winding to supply amplifier *TLV431* and to provide a turn-on signal for synchronous-rectifier turn-off switch Q_{OFF}. Coupling transformer T_C is magnetized by a simple current source consisting of pnp transistor Q_1, resistors R_E, R_{B1}, and R_{B2}, and primary V_{CC} is supplied by auxiliary winding N_S of inductor L_F. The current source is turned on and off by a carrier signal which is synchronized and equal to the main converter switching period T_S, and which has a fixed on time T_A. The demodulator is implemented with a simple peak detector, where diode D_H acts as sampling switch S_H. Finally, sampled error voltage V^*_{EA} is level shifted and inverted, and compared at the PWM modulator to a ramp which is proportional to switch current i_S.

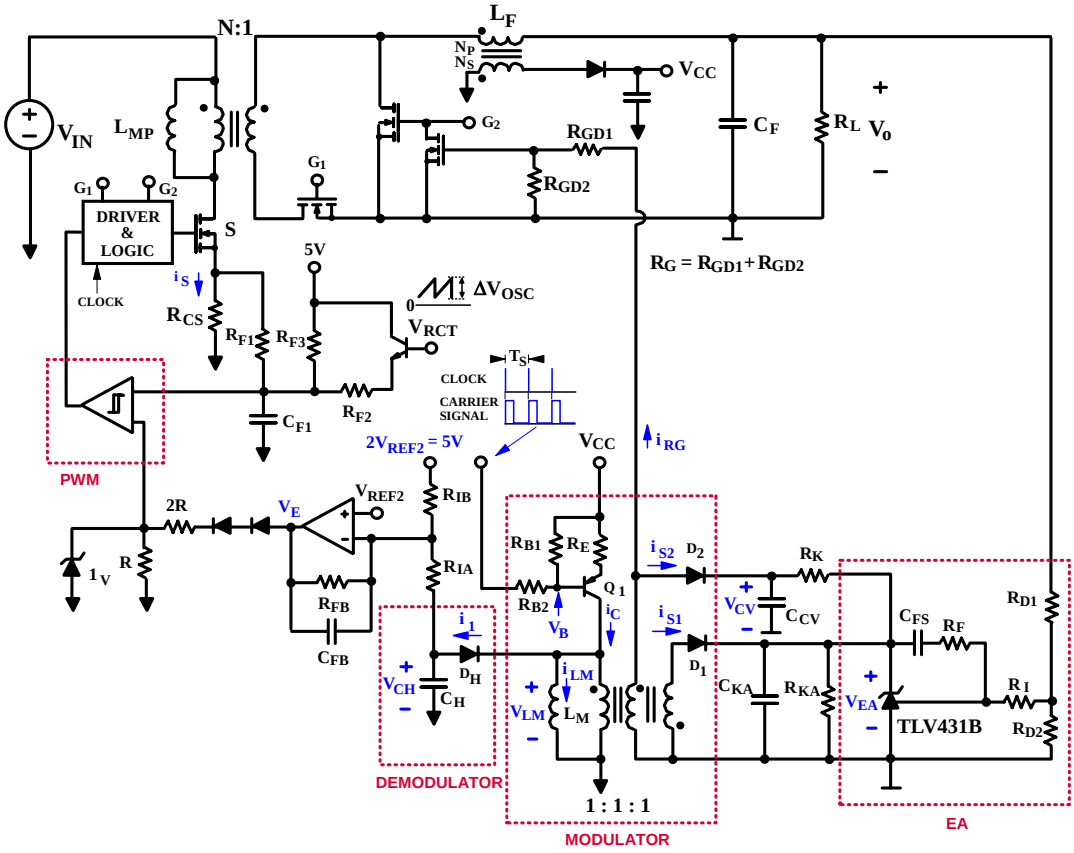

Fig. 3 Circuit diagram of a current-mode controlled forward converter with synchronous rectifiers and AM magnetic feedback implementation

The AM magnetic feedback circuit can be simplified to three topological stages, as shown in Fig. 4, for the case when the current source is on, i.e., when the carrier signal is high as shown in Fig. 4(a), and, when the current source is off, i.e., when the carrier signal is low as shown in Fig. 4(b) and 4(c). Key switching waveforms of a single switching cycle are shown in Fig. 5. While the carrier signal is high, the current source is on, diodes D_H and D_1 are reverse biased, and diode D_2 is forward biased. While diode D_2 is forward biased, voltage V_{LM} across magnetizing inductance L_M is equal to $V_{CV}+V_F$, where V_{CV} is the voltage across capacitor C_{CV}, V_F is the forward voltage drop of diode D_2, and magnetizing current i_{LM} begins to linearly increase from zero. Current i_C then divides between magnetizing inductance L_M, equivalent gate resistor R_G, and diode D_2. Meanwhile, voltage V_{EA}^* across capacitor C_H, which in the previous switching cycle was charged to error voltage V_{EA}, slowly discharges through resistors R_{IA} and R_{IB}. Once the carrier signal goes low, the current source turns off, diodes D_1 and D_H become forward biased, diode D_2 becomes reverse biased, and voltage V_{LM} is equal to $-(V_{EA}+V_F)$. Inductance L_M begins to demagnetize, as shown in Fig. 5. Finally, hold capacitor C_H peak charges to error voltage V_{EA}. Once magnetizing inductance L_M completely demagnetizes, all diodes become reverse biased, and hold capacitor C_H begins to slowly discharge through resistors R_{IA} and R_{IB}, as shown in Fig. 4(c).

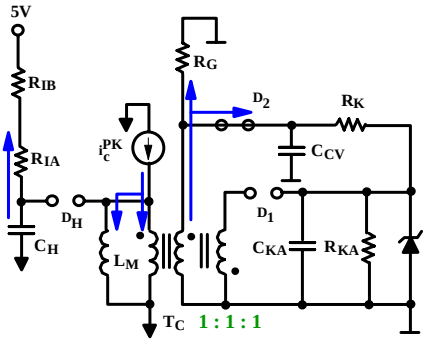

(a) $0 < t < T_A$

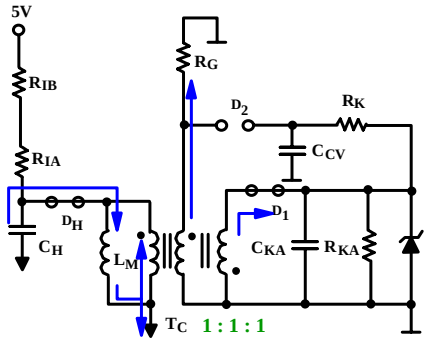

(b) $T_A < t < T_S - T_d$

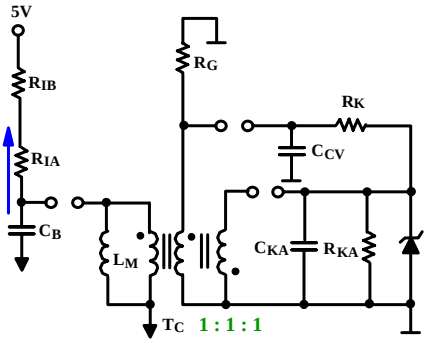

(c) $T_S - T_d < t < T_S$

Fig. 4 Topological stages of AM magnetic feedback implementation where current source i_C^{max} is (a) on (b) off, (c) coupling transformer T_C is completely demagnetized.

IV. Design of AM Magnetic Feedback

A. *Steady-State Design*

In order to continuously sample the error voltage, coupling transformer T_C must be designed with enough margin to prevent saturation. In addition, saturation of current source transistor Q_1 must be avoided so that current i_C is insensitive to current gain h_{FE} of transistor Q_1, since h_{FE} is sensitive to both temperature and tolerance. Finally, error amplifier *TLV431* must have a minimum supply current of 0.1 mA, and a minimum voltage of 1.24V (i.e., V_{EAmin}=1.24V).

To prevent saturation of transistor Q_1, base voltage V_B must be more than one pn diode drop greater than voltage V_{LM}. By selecting a desired maximum voltage level of error voltage V_{EA}, e.g., V_{EAmax}=4V, and by selecting a reasonable value for resistor R_{IB}, e.g., 10k-50kΩ, resistor R_{FB} can be determined

$$R_{FB} = R_{IB}\left(\frac{V_{E\max}}{\Delta V_{EA}}\left(1+\frac{V_{EA\min}}{V_{REF2}}\right)-\frac{V_{E\min}}{\Delta V_{EA}}\left(1+\frac{V_{EA\max}}{V_{REF2}}\right)+1\right), \quad (1)$$

where V_{Emax}=4.2V, V_{Emin}=0V, and $\Delta V_{EA}=V_{EAmax}-V_{EAmin}$. Next,

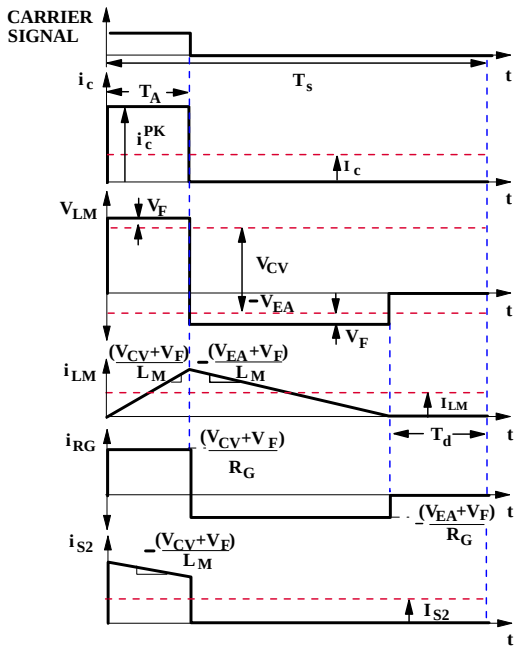

Fig. 5 Key switching waveforms of AM magnetic feedback implementation

resistor R_{IA} and hold capacitor C_H can be calculated

$$R_{IA} = \frac{R_{FB}R_{IB}}{R_{FB} - R_{IB}}\left(1 + \frac{V_{EA\min}}{V_{REF2}}\right), \quad (2)$$

$$C_H = \frac{10T_S}{2\pi(R_{IA} + R_{IB})}, \quad (3)$$

where the value of C_H is a trade-off between a low ripple and excessive delay introduced in the feedback loop.

Voltage V_{CV} can be calculated based on the maximum steady state error voltage V_{EA} and selected coupling transformer dead time T_d and selected current source on time T_A as

$$V_{CV} = -\left(1 - \left(1 - \frac{T_d}{T_S}\right)\frac{T_S}{T_A}\right)(V_{EA} + V_F) - V_F. \quad (4)$$

Next, the required average magnetizing current I_{LM} can be calculated,

$$I_{LM} = \frac{V_{CV} + V_F}{2L_M} T_A\left(1 - \frac{T_d}{T_S}\right). \quad (5)$$

From the minimum *TLV431* current, average diode current I_{S2} can be selected, resistor R_K can be calculated,

$$R_K = (V_{CV} - V_{EA})/I_{S2}, \quad (5)$$

and average diode current $I_{S1}+I_1$ can be calculated as

$$I_{S1} + I_1 = -\frac{V_{CV} + V_F}{V_{EA} + V_F}\frac{T_A}{T_S}\left(\frac{-(V_{CV} + V_d)T_A}{2L_M} + \frac{V_{KA} + V_d}{R_{GD}}\right). \quad (6)$$

The required average collector current I_C can now be determined since

$$I_C = I_{S2} - I_{S1} - I_1 + I_{LM}, \quad (7)$$

and finally, the peak collector current i_c^{pk} can be determined as

$$i_c^{pk} = I_C T_S / T_A. \quad (8)$$

Since saturation of transistor Q_1 must be avoided, base voltage V_B should be set approximately two volts higher than voltage $V_{CV}+V_F$. Resistor R_E can then be calculated,

$$R_E = \frac{V_{CC} - V_B - V_{ebf}}{i_c^{pk}(1 + 1/h_{FE})}, \quad (9)$$

where voltage V_{ebf} is the base-emitter voltage of Q_1. It should be noted that voltage V_{CC}, which should be selected greater than voltage V_B, may be excessively high based on the selection of maximum error voltage V_{EAmax}. Additional iterations may be needed to find both the optimal value of voltages V_{EAmax} and V_{CC}. By selecting a reasonable value of base resistor R_{B2}, e.g. 1k-10kΩ, base resistor R_{B1} can be calculated assuming that current gain h_{FE}>>1,

$$R_{B1} = R_{B2}(1 - V_B/V_{CC}). \quad (10)$$

B. *Small-Signal Design*

A small-signal block diagram of a converter operating with current-mode control, originally proposed in [8], is shown in Fig. 6, whereas the transfer functions are given in Table 1. Current loop T_i is defined as the product of power stage transfer function G_{id}, equivalent sensing resistor R_S, sampling gain H_e, and modulator gain F_M, i.e.,

$$T_i = G_{id} R_S H_e F_M, \quad (11)$$

whereas voltage loop T_v is defined as the product of control-to-output transfer function G_{vc}, sensing gain K_d, error amplifier transfer function G_{EA}, sample and hold transfer function G_{SH}, and transfer function G_E, i.e.,

$$T_v = G_{vc} K_d G_{EA} G_{SH} G_E. \quad (12)$$

Transfer function G_{vc} is the control-to-output transfer function of the power stage with current loop T_i closed, i.e.,

$$G_{vc} = \frac{\hat{v}_o}{\hat{v}_c} = \frac{F_M G_{vd}}{1 + T_i} \approx \frac{G_{vd}}{R_S G_{id}} = \frac{R_L}{R_S}\frac{1 + s/\omega_{zc}}{1 + s/\omega_P}\Bigg|_{T_i >> 1}. \quad (13)$$

Generally, subharmonic oscillation can occur in designs which have a duty cycle greater than or equal to 50%. However, this can be overcome by a proper selection of compensation ramp S_e as discussed in [8].

The design of error amplifier G_{EA} is based on transfer functions G_{vc}, K_d, G_{SH}, and G_E, and straight-line approximations are shown in Fig. 7. It is beneficial to include capacitor C_{FB} across feedback resistor R_{FB} for noise immunity, which introduces an additional pole (f_{p1}) that should be placed well below switching frequency f_S. In fact, pole f_{p1} can be used to cancel esr zero f_{zc} of control-to-output transfer function G_{vc}. In addition, it should be noted that sample and hold transfer function G_{SH} introduces a phase-delay which should be considered before finalizing the loop design.

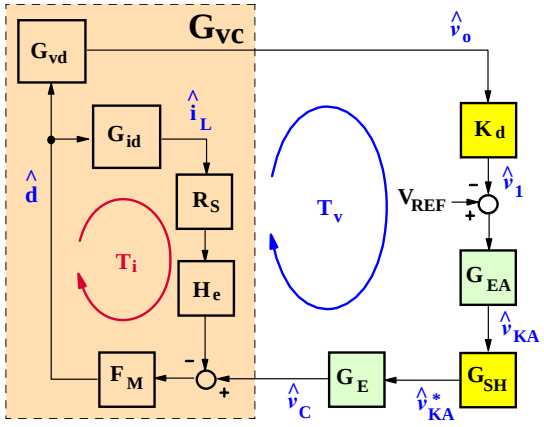

Fig. 6 Small-signal block diagram of forward converter with current-mode control and magnetic feedback.

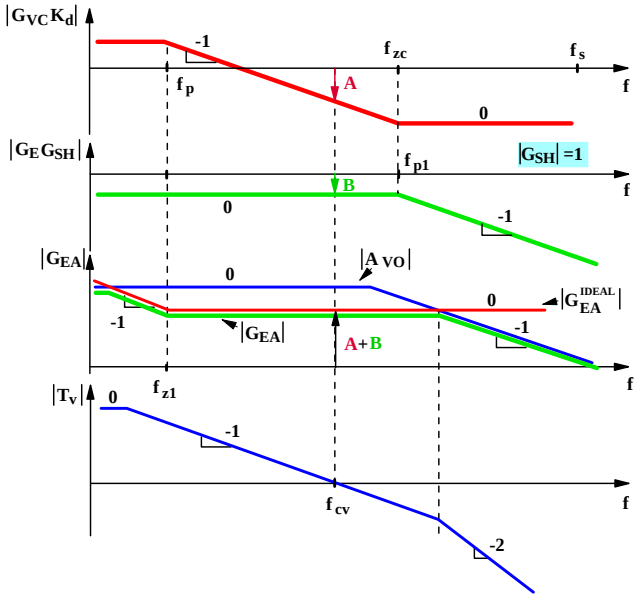

Fig. 7 Compensation of voltage loop using pole-zero cancellation and straight-line approximations.

Design of loop gain T_V should be done at full load since pole f_P of control-output transfer function G_{vc} increases as load resistor R_L decreases, thereby resulting in the maximum crossover frequency. Selection of crossover frequency f_{CV} should be well below switching frequency f_S, i.e., $f_{CV} << f_S$. In fact, crossover frequency f_{CV} may be further limited due to the low open loop gain A_{VO} of TLV431. Finally, crossover frequency f_{CV} is further limited by the sample and hold delay.

From Fig. 7, an integrator is needed to provide a high gain at low frequencies for good load regulation, while zero f_{z1} is needed to cancel out control-to-output transfer function pole G_{vc}. Switching ripple is attenuated by both pole f_{p1} of transfer function G_E, and by open loop gain A_{VO} of TLV431.

$$\left|G_{EA}(f=f_{CV})\right| = \frac{1}{\underbrace{\left|K_d G_{vc}(f=f_{CV})\right|}_{A} \cdot \underbrace{\left|G_E(f=f_{CV})\right|}_{B}}, \qquad (14)$$

where the gain of sample-hold transfer function G_{SH} is equal to unity. Since $f_{CV} > f_{z1}$,

$$\left|G_{EA}(f=f_{CV})\right| = \frac{R_F}{R_I}. \qquad (15)$$

By selecting feedback resistor R_F within a reasonable range (e.g., 50-200k), resistor R_I can be calculated,

$$R_I = R_F AB. \qquad (16)$$

By setting zero f_{z1} equal to pole f_P, capacitor C_{FS} can be calculated,

$$C_{FS} = \frac{1}{2\pi R_F f_{z1}}. \qquad (17)$$

Once compensation components are calculated, error amplifier transfer function G_{EA} should be checked with open-loop gain A_{VO} included to see if the design is optimal. Generally, open-loop gain A_{VO} changes with dc operating

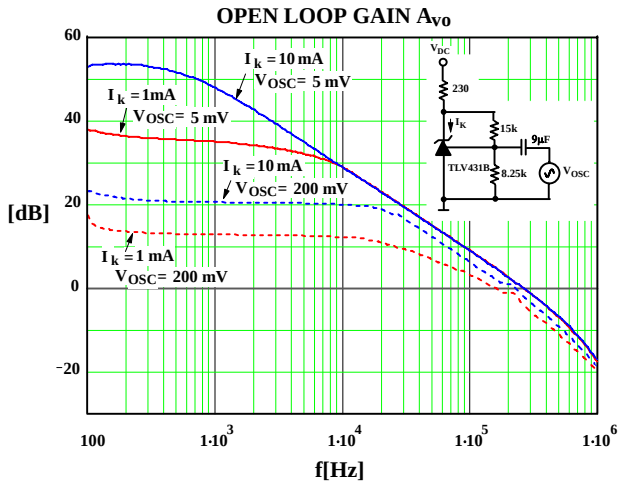

Fig. 8 Measurements of open-loop gain A_{VO} of TLV431B using datasheet recommended test circuit.

current I_K as well as the amplitude of input signal V_{OSC}, as shown in Fig. 8. It should be noted that the test circuit was obtained from the TLV431B ON Semiconductor datasheet. Figure 9 shows the measured open loop gain including capacitor C_{KA}, resistor R_{KA}, and R_K replaced with a 3-kΩ resistor.

V. Experimental Results

To validate the design procedure, a 7-V/15-W lab prototype of a forward converter with magnetic feedback and amplitude modulation was designed for an input voltage range $35 < V_{IN} < 72$, and an ambient operating range of -40 to 100 °C. The key component values are shown in Fig. 10.

In the experimental circuit, maximum error voltage V_{EAmax} was selected as 4 V, and the minimum cathode current I_k of TLV431 was set to 4 mA. On-time T_A of current source i_C was set to 500 nsec, and feedback transformer dead time T_d was designed to be half of switching period T_S. As a result, voltage V_{CV} was approximately 11.5 V, and base voltage V_B of transistor Q_1 was set approximately 2-V higher, ensuring that

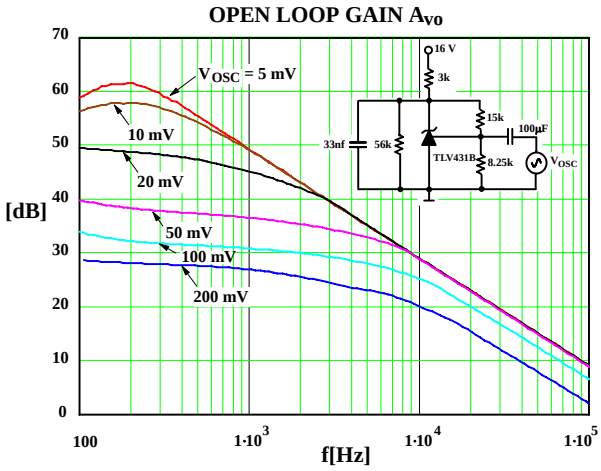

Fig. 9 Measurements of open-loop gain A_{VO} of TLV431B including resistor R_{KA}, capacitor C_{KA}, and R_K = 3kΩ.

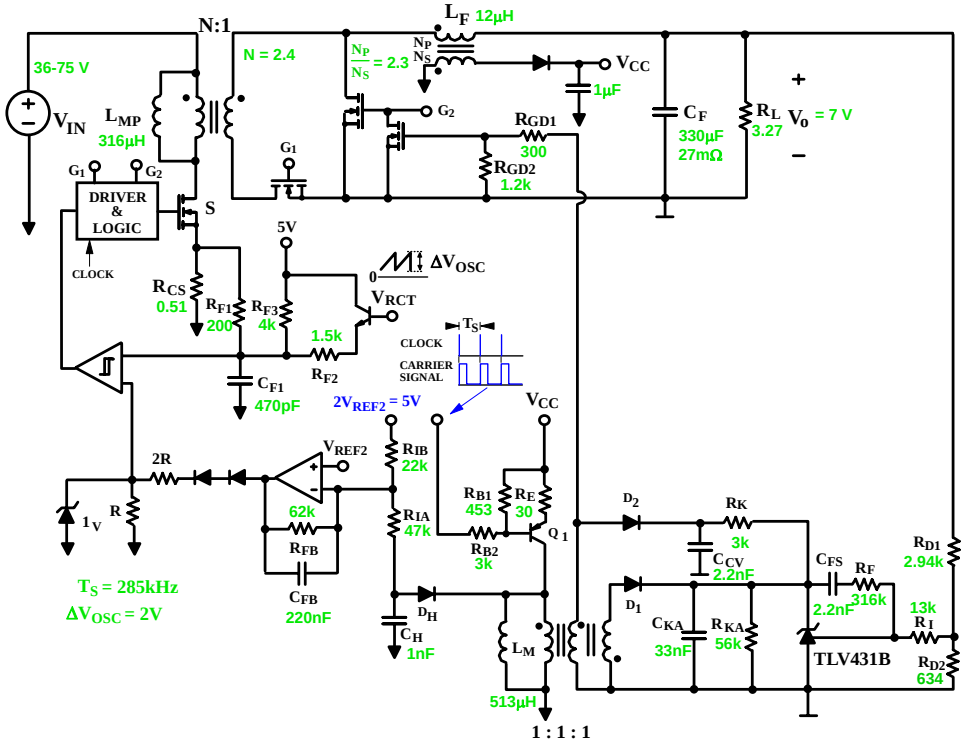

Fig. 10 Circuit diagram and key component values of 7-V/15-W experimental prototype

transistor Q_1 does not saturate. This required voltage V_{CC} to be greater than 13.5 V, and, therefore, V_{CC} was set to 16 V. Finally, the carrier frequency was set equal to switching frequency f_s, where f_s = 285 kHz.

Figure 11 shows oscillograms of two different control designs of the experimental prototype. In Fig. 11(a), current source transistor Q_1 was designed to operate in the saturation region (i.e., voltage V_{CV} > base voltage V_B), and in Fig. 11(b), current source transistor Q_1 was designed to operate in the active region. For both designs, dead time T_d was compared at room and high ambient temperature. Figure 11(a) shows that on-time T_A of the current source is significantly longer at high ambient temperature than at room ambient temperature. This is due to the fact that on-time T_A is dependent on current gain h_{FE} of transistor Q_1 when Q_1 operates in the saturation region. As a result, the magnetizing energy of coupling transformer T_C increases, and decreases dead-time T_d. As the ambient temperature increases, dead time T_d decreases until it reaches zero, which results in the loss of output-voltage feedback.

Figure 11(b) shows that on-time T_A is nearly constant because transistor Q_1 operates in the active region. Generally, on-time T_A is independent of current gain h_{FE} when transistor Q_1 operates in the active region.

A comparison between the measured and calculated loop gain is shown in Fig. 12, which demonstrates a 6-kHz bandwidth, 60-degrees phase margin, and 20-dB gain margin. The open-loop gain A_{VO} was measured using the test circuit shown in Fig. 9 for an oscillation input of 50-mV, and used in the voltage loop gain calculations.

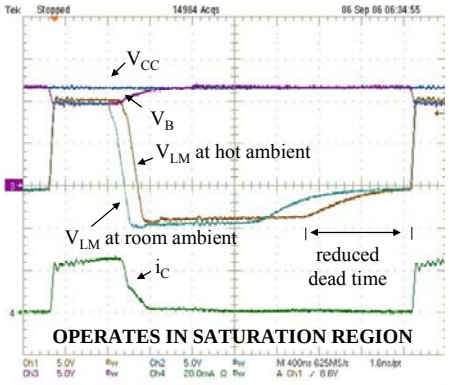

Fig. 11 Experimental results of a 7-V/15-W lab prototype at room and hot ambient for transistor Q_1 operating in the (a) saturation region (b) active region.

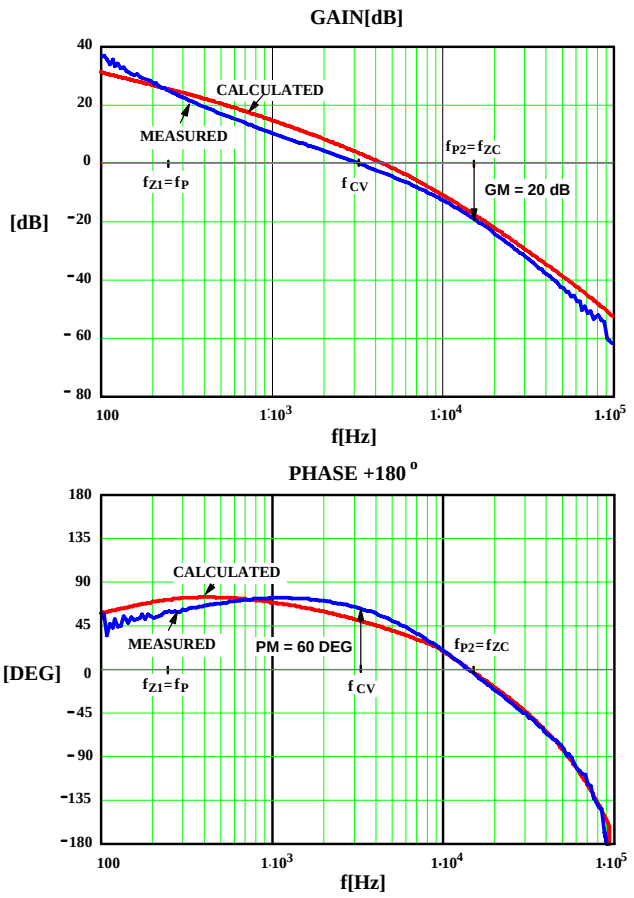

Fig. 12 Measured vs. calculated voltage loop gain at full load and nominal input voltage.

Generally, it is desirable to have a crossover frequency greater than one-tenth of switching frequency f_s. At one-tenth of switching frequency f_s, the phase lag due to the sample and hold is 36-degrees, permitting at best a phase margin less than 54-degrees assuming that the voltage-loop gain crosses 0-dB with a -1 slope. It was found that although switching frequency f_s was set very high (i.e., f_s=285 kHz), to achieve a phase margin greater than 45-degrees, the voltage-loop crossover frequency was limited to less than 10-kHz by the low open-loop gain of TLV431.

VI. Summary

A forward converter with magnetic feedback and amplitude modulation was thoroughly analyzed, and a comprehensive steady-state and small-signal design procedure was presented. The design procedure was verified with a 7-V/15-W experimental prototype, and steady-state and small-signal measurements were provided.

References

[1] M.P. Sayani, R.V. White, D.G. Nason, and W.A. Taylor, "Isolated feedback for off-line switching power supplies with primary-side control," *IEEE Applied Power Electronics Conf. (APEC) Proc.*, pp. 203-211, Feb. 1988.

[2] B. Mammono, "Isolating the control loop," in *Unitrode Seminar Proc.*, 1997, pp. C-21-C-15.

[3] K. Billings, "Switchmode power supply handbook", New York: McGraw-Hill Inc., 1989, pp.3.161-3.165.

[4] J. Bliss, "Theory and characteristics of phototransistors," Motorola Application Note AN-440, Motorola Databook "*Optoelectonics device data*", pp. 9.3-9-13, 1989.

[5] Y. Panov and M.M. Jovanovic, "Small-signal analysis and control design of isolated power supplies with optocoupler feedback," *IEEE Transactions on Power Electronics*, vol.20, no.4, pp.823-832, July 2005.

[6] L. Ou and D. Curtis, "Magnetic feedback ranks high in military converters," *Power Electronics Technology*, pp. 14-19, July 1995.

[7] R. Valley, "The uc1901 simplifies the problem of isolated feedback in switching regulators," *TI Application Note* U-94.

[8] R.B. Ridley, "A new, continuous-time model for current-mode control", *IEEE Transactions on Power Electronics*, vol.6, no.2, pp.271-280, April 1991.

TABLE 1 : KEY SMALL-SIGNAL TRANSFER FUNCTIONS

$G_{vd} = \frac{\hat{v}_o}{\hat{d}} = \frac{V_{IN}}{N} \frac{1+\frac{s}{\omega_{zc}}}{1+\frac{1}{Q}\frac{s}{\omega_o}+\frac{s^2}{\omega_o^2}}$	$F_M = \frac{\hat{d}}{\hat{v}_c} = \frac{1}{(S_N + S_e)T_S}$	$G_{EA} = \frac{\hat{v}_{EA}}{\hat{v}_1} = \frac{\omega_I(1+s/\omega_{z1})}{s} \frac{1}{1+\frac{1}{A_{vo}\beta}}$	$H_e = 1+\frac{1}{Q_z}\frac{s}{\omega_n}+\frac{s^2}{\omega_n^2}$
$G_{id} = \frac{\hat{i}_L}{\hat{d}} = \frac{V_{IN}}{NR_L} \frac{1+\frac{s}{\omega_{z2}}}{1+\frac{1}{Q}\frac{s}{\omega_o}+\frac{s^2}{\omega_o^2}}$	$K_d = \frac{\hat{v}_1}{\hat{v}_o} = \frac{R_{D2} \parallel R_I}{R_{D2} \parallel R_I + R_{D1}}$	$G_E = \frac{\hat{v}_c}{\hat{v}_{EA}^*} = \frac{1}{3}\frac{R_{FB}}{R_{IA}} \frac{1}{1+s/\omega_{FB}}$	$G_{SH} = e^{-sT_S}$
$\omega_{zc} = \frac{1}{r_c C_F}$ $\omega_{z2} = \omega_P = \frac{1}{R_L C_F}$ $Q = \frac{1}{\omega_o}\frac{1}{C_F r_c + L_F/R_L}$ $S_N = \frac{-V_O + V_{IN}/N}{L_F}\frac{R_{cs}}{N}$ $S_e = \frac{V_{IN}}{L_{MP}}R_{cs} + \frac{\Delta V_{osc}}{T_S}\frac{R_{f1}}{R_{f1}+R_{f2}}$			
$\omega_o = \frac{1}{\sqrt{L_F C_F}}$ $\omega_{FB} = \frac{1}{R_{FB}C_{FB}}$ $\omega_n = \pi/T_S$ $Q_z = -2/\pi$ $\omega_I = \frac{1}{R_I C_{FS}}$ $\omega_{z1} = \frac{1}{R_F C_{FS}}$ $R_S = R_{CS}/N$ $\beta = \frac{sC_{FS}R_I}{1+sC_{FS}(R_I+R_F)}$			